

DECEMBER 01 2025

Directional active noise control for drone noise reduction

Hanwen Bi  ; Yile (Angela) Zhang  ; Thushara D. Abhayapala  ; Prasanga N. Samarasinghe 



JASA Express Lett. 5, 124801 (2025)

<https://doi.org/10.1121/10.0039953>



View
Online



Export
Citation

Articles You May Be Interested In

Frequency band analysis and comparison of localisation techniques for drones using microphone array measurements

JASA Express Lett. (February 2025)

Acoustic localization and tracking of a multi-rotor unmanned aerial vehicle using an array with few microphones

J. Acoust. Soc. Am. (September 2020)

Lightweight deep convolutional neural network for background sound classification in speech signals

J. Acoust. Soc. Am. (April 2022)

Directional active noise control for drone noise reduction

Hanwen Bi,^{a)}  Yile (Angela) Zhang,  Thushara D. Abhayapala,  and Prasanga N. Samarasinghe 

School of Engineering, The Australian National University, Canberra, Australian Capital Territory 2600, Australia

Abstract: Drones have become essential tools for applications ranging from aerial surveillance to last-mile delivery, raising concerns about noise pollution in populated environments. This paper presents a directional active noise control (ANC) framework that targets far-field noise reduction, rather than local suppression. A virtual microphone-based ANC algorithm is employed, using a near-drone microphone array to attenuate noise in a specific region. Experiments in a semi-anechoic chamber show an average reduction of 4.78 dB in the 1500–2400 Hz band and up to 10 dB at harmonic frequencies, highlighting the promise of directional ANC for quieter drone operations in sensitive settings. © 2025 Author(s). All article content, except where otherwise noted, is licensed under a Creative Commons Attribution (CC BY) license (<https://creativecommons.org/licenses/by/4.0/>).

[Editor: Wen Xu]

<https://doi.org/10.1121/10.0039953>

Received: 4 August 2025 Accepted: 9 November 2025 Published Online: 1 December 2025

1. Introduction

Small-scale unmanned aerial vehicles (UAVs), commonly known as drones, have become increasingly popular for applications such as food and parcel delivery (Chiang *et al.*, 2019), mapping (Ventura *et al.*, 2016), search and rescue (Mishra *et al.*, 2020), and wildlife surveys (Jones *et al.*, 2006). Despite the growing importance of drones, the noise pollution from them is strong and can affect daily life and the health of residents. Due to the high-frequency component, drone noise might be perceived as more annoying than road vehicles (Christian and Cabell, 2017). Therefore, effective drone noise mitigation strategies are crucial to supporting the sustainable integration of drones into everyday life.

Drone noise reduction methods can be broadly categorized into passive and active approaches. Passive noise reduction focuses on modifying the design and materials of propellers, motors, and airframes to reduce noise. Techniques include optimising propeller and fuselage geometry (Gur and Rosen, 2009), using ducted propellers, and adding sound-absorptive barriers (Miljkovic, 2018). However, these methods are generally less effective for low-frequency noise (Everest and Pohlmann, 2022). In contrast, active drone noise reduction methods actively counteract and mitigate noise emissions during flight operations. These approaches can be further divided into phase control and active noise control (ANC). Phase control technique reduces noise by adjusting the relative angular blade positions of multiple propellers, thereby minimising noise levels in specific target areas (Schiller *et al.*, 2019). However, this method is limited to cancelling specific harmonics of tonal noise (Bi *et al.*, 2021). ANC, on the other hand, employs secondary sources (loudspeakers) to generate anti-noise that destructively interferes with the primary noise (Elliott and Nelson, 1993). ANC allows for noise cancellation in a controllable region, and with a sufficient number of secondary sources, noise can be effectively mitigated. This makes ANC a highly flexible and promising approach for drone noise reduction.

The current research on drone ANC is limited, with only a few studies addressing this topic. Kusni (2002) initially proposed a propeller noise reduction system that effectively reduced tonal noise over a circular target region based on simulations. However, this approach required multiple secondary sources for each propeller, making it impractical for drone applications. Similarly, Dubravko introduced a multichannel ANC system using 12 loudspeakers positioned around each propeller to cancel the noise of the propeller, but the concept remained theoretical, lacking both simulation and experimental validation (Miljkovic, 2018). Narine (2020) implemented a preliminary single-channel ANC system targeting the tonal noise generated by a single propeller. However, the system was designed to cancel noise at a single spatial point near the propeller using a loudspeaker positioned at a long distance from the propeller, making the setup impractical for use on a flying drone. Bi *et al.* proposed a narrow-band directional ANC system designed to reduce drone noise propagating downward. While effective, this system required a speaker and microphone array arranged in a spherical sector shape, limiting its practical implementation (Bi *et al.*, 2022; Bi *et al.*, 2023). Recently, Steiner *et al.* (2025) conducted a controlled indoor experiment to study UAV ANC and measuring and modelling the acoustic transfer paths needed for ANC filter design. However, their results focused on optimising a fixed-point scenario, which can reduce the sound pressure level by

^{a)}Corresponding author: hanwen.bi@anu.edu.au

9 dB at a single location. Despite these efforts, most drone ANC research has certain limitations: (i) focusing solely on propeller noise, neglecting other sources of drone noise; (ii) targeting only narrow-band cancellation; (iii) lacking experimental validation.

To address these research gaps, this paper proposes and experimentally validates a directional ANC system for drones. Given the loading and power constraints of drones, fully cancelling all outgoing noise would require an impractically large number of secondary sources. Instead, to minimise disturbances to nearby residents, this work focuses on drone noise reduction in a directional far-field region based on the near-field measurement from an on-board microphone array. Since deploying microphones in the far-field region is impractical, the proposed system incorporates the virtual microphone ANC algorithm from (Abhayapala *et al.*, 2023), which enables noise reduction in the target region using only near-field measurements. The algorithm is detailed in Sec. 3. The main contribution of this paper is twofold:

- We present a drone ANC system capable of cancelling broadband noise (1500–2400 Hz) over a far-field region.
- To the best of our knowledge, we provide the first experimental evaluation of a drone ANC system's performance in the far field.

2. Problem formulation

Consider a drone ANC system as shown in Fig. 1. The drone is the primary noise source with J reference sensors placed near its propellers. Let there be Q monitoring microphones hanging on the drone to physically measure the near-field drone noise and V virtual microphones sampling the region of interest (ROI) in the far-field. L secondary sources are mounted on the drone fuselage, between the drone and the monitoring microphone, to control the noise propagating towards the ROI. Figure 1(a) shows a scenario where the drone flies over a residential area; in this case, the goal is to suppress noise directed downward towards the ground. Figure 1(b) illustrates an urban environment with high-rise buildings, where the objective is to reduce lateral noise propagation towards surrounding structures.

In the short-time Fourier transform (STFT) domain, we can represent the monitoring microphone signals and virtual microphone signals as

$$\mathbf{e}_M(f, t) = \mathbf{P}_M(f) \mathbf{x}(f, t) + \mathbf{S}_M(f) \mathbf{y}(f, t), \quad (1)$$

$$\mathbf{e}_V(f, t) = \mathbf{P}_V(f) \mathbf{x}(f, t) + \mathbf{S}_V(f) \mathbf{y}(f, t), \quad (2)$$

where $\mathbf{e}_M(f, t)$ denotes the $Q \times 1$ monitoring microphone signals, $\mathbf{e}_V(f, t)$ represents the $V \times 1$ virtual microphone signals, $\mathbf{x}(f, t)$ is the reference signals with the size of $J \times 1$, $\mathbf{y}(f, t)$ is the secondary source signals with the size of $L \times 1$, \mathbf{P}_M and \mathbf{S}_M are the primary channel response matrices and the secondary channel response matrices to monitoring microphones of sizes $Q \times J$ and $Q \times L$, respectively. \mathbf{P}_V and \mathbf{S}_V are the primary channel response matrices and the secondary channel response matrices to virtual microphones of sizes $V \times J$ and $V \times L$, respectively.

Since measurements from virtual microphones are not directly accessible, the research problem becomes how to derive an adaptive ANC algorithm that iteratively updates \mathbf{y} based on the available information from \mathbf{x} , with the objective of minimising the residual noise observed at the virtual microphone positions, represented by \mathbf{e}_V .

3. Drone ANC algorithm

In this section, we introduce the algorithm used in the drone directional ANC system.

The ANC algorithm has two stages, the tuning stage and the control stage. In the tuning stage, which can be done in the drone factory before launching to the market, the drone hovers at a certain height, and secondary sources play

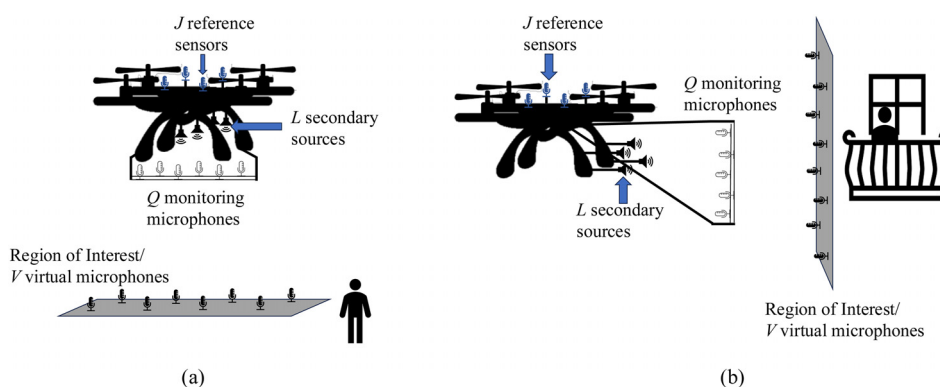


Fig. 1. Drone directional ANC system setup (a) reducing noise downward and (b) reducing noise sideward: Q monitoring microphones hanging on the drone, L secondary sources mounted on the drone fuselage, J reference sensors placed near the drone propellers, and V virtual microphones sample the ROI in the far-field.

white noise. We place physical microphones at both the monitoring microphone and virtual microphone positions to measure \mathbf{e}_M and \mathbf{e}_V . Then, we calculate the relative transfer matrix (ReTM) between \mathbf{e}_M and \mathbf{e}_V , denoted as R_{VM} . The ReTM is defined as the spatial mapping between the two microphone groups arbitrarily distributed within a given spatial region (Abhayapala *et al.*, 2023). Note that the ReTM is independent of the source signals and is solely determined by the spatial properties (i.e., the acoustic transfer functions) of the acoustic environment, the source positions, and the microphone positions. Therefore, if the drone's operating environment and the relative positions between the drone and the monitoring and virtual microphones do not change, the ReTM between \mathbf{e}_M and \mathbf{e}_V remains constant. R_{VM} can be estimated by (Abhayapala *et al.*, 2023)

$$R_{VM}(f) \approx P_{VV}(f) P_{MV}^\dagger(f), \quad (3)$$

where $(\cdot)^\dagger$ denotes the Moore–Penrose pseudo-inverse, $P_{VV}(f) \triangleq \mathbb{E}\{\mathbf{e}_V(f, t)\mathbf{e}_V^*(f, t)\}$ is the auto-correlation matrix, $P_{MV}(f)$ is the cross-correlation matrix, which can be calculated by $P_{MV}(f) \triangleq \mathbb{E}\{\mathbf{e}_M(f, t)\mathbf{e}_V^*(f, t)\}$. \mathbb{E} is the expectation obtained by averaging over T time frames, and $(\cdot)^*$ denotes the conjugate transpose. With R_{VM} , we can estimate the far-field noise over the ROI by the onboard microphone measurements through

$$\mathbf{e}_V(f, t) = R_{VM}(f) \mathbf{e}_M(f, t). \quad (4)$$

In the control stage, we assume the R_{VM} stays unchanged from the tuning stage and use Eq. (4) to estimate \mathbf{e}_V from \mathbf{e}_M . Note that R_{VM} corresponding to different operating conditions (e.g., drone altitudes, orientations, or environment) can be pre-estimated and stored. During operation, the system selects the most appropriate R_{VM} according to the current condition before continuing the adaptive filter update. This strategy is conceptually analogous to the selective fixed-filter approaches in ANC (Shi *et al.*, 2022; Luo *et al.*, 2024), where pre-calculated filters are used to accommodate varying acoustic scenarios efficiently.

The anti-noise loudspeaker signal is computed as

$$\mathbf{y}(f, t) = \sum_j \mathbf{W}_j^T(f, t) * \mathbf{x}'_j(f, t), \quad (5)$$

where $\mathbf{x}'_j(f, t)$ represents the jth reference signal $\mathbf{x}_j(f, t)$ filtered by the secondary path model to the monitoring microphone array $S_M(f)$ and the estimated ReTM $R_{VM}(f)$. Then, by integrating ReTM within the conventional FxLMS adaptive ANC algorithm (Kuo and Morgan, 1996), the update equation is given by (Zhang *et al.*, 2024)

$$\mathbf{W}_j(f, t+1) = \mathbf{W}_j(f, t) - \mu \mathbf{x}_j(f, t) R_{VM}^H(f) S_M^H(f) \mathbf{e}_M(f, t) R_{VM}(f), \quad (6)$$

where \mathbf{W}_j is the $L \times 1$ adaptive filter and μ is the step size.

4. Experiments

In this section, we evaluated the proposed drone ANC system with practical experiments conducted in a semi-anechoic acoustic chamber at the Australian National University with dimensions of 6.2 m \times 4.8 m \times 3.2 m and $T_{60} = 0.126$ s.

4.1 Experiment setup

A quadrotor UAV with a diagonal size of 32 cm was used for the experiment. A 16-channel UMA-16 microphone array (13.2 cm \times 13.2 cm) was employed to monitor the near-field sound field, while a 9-channel microphone array (36 cm \times 36 cm) was used to measure the sound field over the ROI. Four MEMS microphone chips served as reference microphones. The ND20FA-6 loudspeakers from DAYTON AUDIO (Springboro, OH), with a diameter of 4 cm, were used as the secondary sources.

We set $J = 4$ reference sensors, $L = 4$ secondary sources, $Q = 16$ monitoring microphones, and $V = 9$ virtual microphones. We consider the 16-channel microphone array and the 9-channel microphone as the monitoring microphone group and virtual microphone group, respectively. Figure 2 shows the experimental setup. The drone was mounted on a 150 cm wooden bar to remain fixed in position. The centers of the two microphone arrays are aligned vertically with the drone, positioned at the same height, and placed horizontally at 40 cm and 300 cm from the drone, respectively. Given the 300 cm separation from the drone, the second microphone array can be reasonably assumed to lie in the acoustic far-field for the mid-frequency of interest. The four reference microphones were placed at each of the four propellers, and the four secondary sources were positioned between the drone fuselage and the monitoring microphone array.

4.2 Experiment procedure

We recorded two 40-s clips of the drone propeller noise under identical experimental conditions at a sampling rate of 48 kHz. Each recording was first filtered using a bandpass filter between 1500 Hz and 2400 Hz (the justification for this sub-band is provided in the following) and then transformed using STFT for ANC analysis. From each 40-s recording, we extracted a 30-s segment and combined the two segments, hereafter referred to as the tuning data. This was used to compute the ReTM between the monitoring and virtual microphone groups via Eq. (3). The calculated ReTM and the

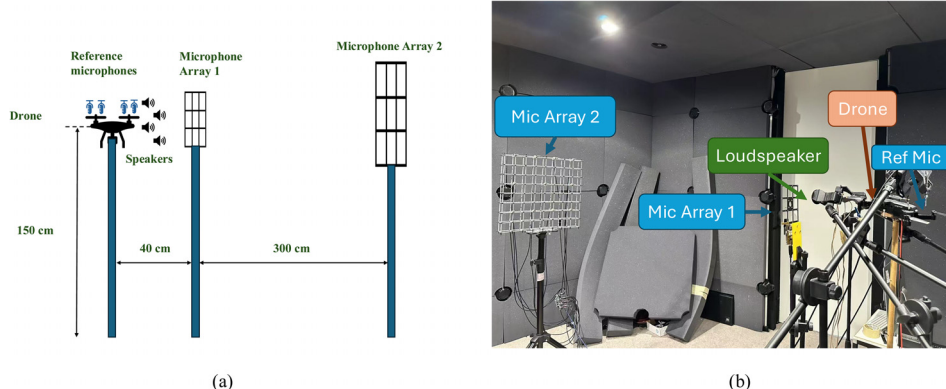


Fig. 2. Drone directional ANC system experiment setup (a) experiment layout (b) experiment photo.

measured monitoring microphone signals were then used to estimate the virtual microphone signals during the ANC control stage. The remaining 8-s segments from each recording, that were not used for tuning data, were combined to form the testing data and subsequently used to evaluate ANC performance. We applied a constant step size $\mu = 0.03$ in the FxLMS algorithm and report preliminary noise reduction results in both the frequency and time domains.

4.3 Justification for sub-band processing

To determine an effective ANC frequency range, we examined the drone noise characteristics from Fig. 3(a) and observed that the blade passage frequencies were particularly prominent in the mid-frequency range of 1200–2400 Hz. Additionally, the magnitude response of the ND20FA-6 loudspeaker was found to be approximately flat within this range, as shown in Fig. 3(b). In contrast, the response below 1500 Hz decreases rapidly, making it unsuitable for low-frequency ANC applications due to insufficient speaker performance. Low-frequency sounds have long wavelengths, requiring a larger cone to move enough air to produce them, which makes it difficult for small-sized speakers to perform well at low frequencies. Given the combined considerations of noise dominance and loudspeaker characteristics, we restricted the ANC processing to this 1500–2400 Hz sub-band to improve ANC efficiency. Note that the optimal ANC frequency range may vary depending on the specific drone and speaker hardware.

4.4 Experiment results

Figures 4(a) and 4(b) show the time-domain error signals at one of the virtual microphones for the tuning and testing data, respectively. Note that the signals have been bandpass filtered to show only the activity within the ANC frequency range. In Fig. 4(a), we show the ANC performance when the noise field in the control stage is the tuning data (the recording used to calculate ReTM). The system achieves an average noise reduction of -5.63 dB, with the error signal converging to a stable level within approximately 3 s. In Fig. 4(b), we present a more realistic scenario, where the noise field during

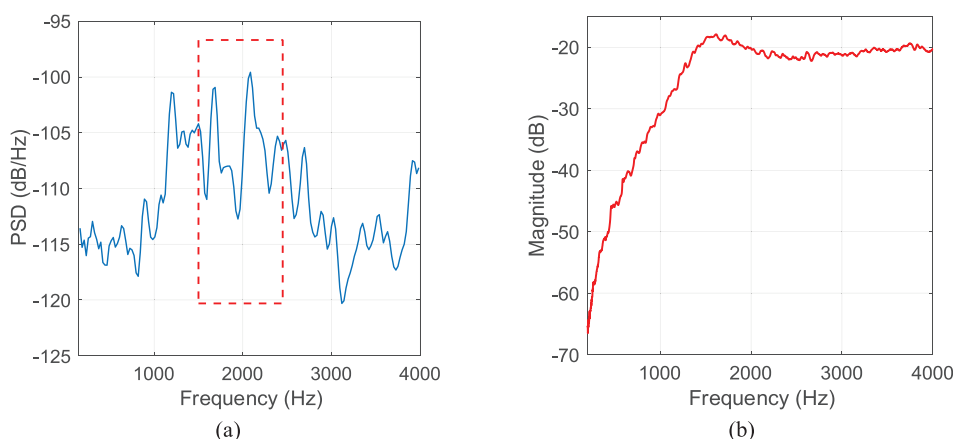


Fig. 3. Justification for sub-band processing: (a) PSD with an arbitrary reference observed at the virtual microphone, showing dominant blade-passage frequency components in the 1500–2400 Hz range. (b) Measured magnitude response (with an arbitrary reference) of the ND20FA-6 loudspeaker, exhibiting a flat response above 1500 Hz and a noticeable roll-off below.

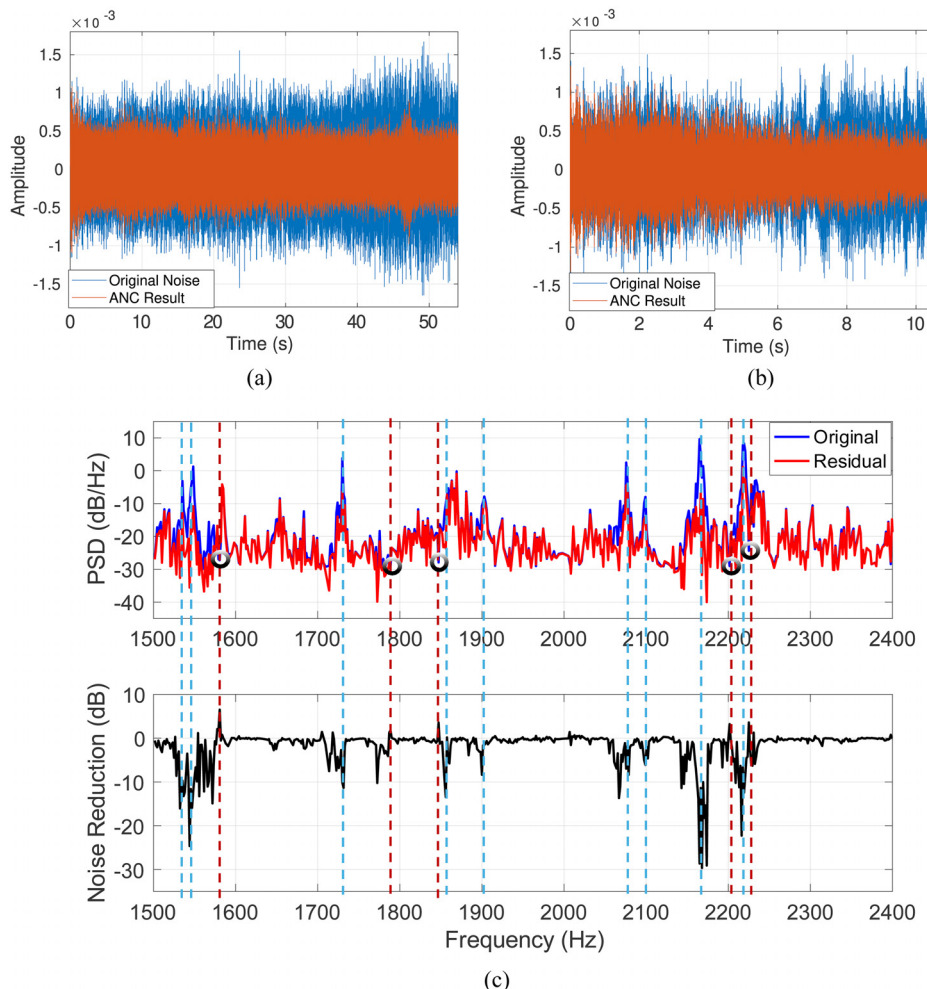


Fig. 4. **Drone ANC results in the time and frequency domains.** (a) **Tuning data:** ANC performance using the same noise recording as in the tuning stage. (b) **Testing data:** performance using a different segment of the noise recording. (c) **PSD with an arbitrary reference and noise reduction at one of the virtual microphones with testing data,** demonstrating approximately 10 dB attenuation within the target frequency band. The red dotted lines indicate positive noise reduction values, which occur where the original noise level was very low.

the control stage is the ANC testing set. Here, the ANC system achieves an average noise reduction of -4.78 dB, with convergence occurring around 5 s.

Figure 4(c) illustrates the power spectral density (PSD) and the corresponding noise reduction at a virtual microphone. The system achieves around 10 dB reduction at the dominant blade passage frequencies, highlighted by the blue dotted lines, which are the most prominent and perceptually significant components of drone noise (Intaratep *et al.*, 2016). At frequencies marked with red dotted lines, slight positive reduction values appear. However, the original noise levels at these frequencies are already low from around -25 to -30 dB (black circles), making even small residuals appear as an increase. The residual noise remains around -20 dB, indicating that the remaining noise is minimal and unlikely to be perceptible in typical environments. The cancellation results and recordings can be viewed online.¹

5. Conclusion

In this work, we propose a directional ANC framework to mitigate drone noise propagating towards predefined far-field regions, addressing urban noise pollution concerns. Through the use of a ReTM-based virtual microphone ANC algorithm, the system can suppress far-field drone noise using monitoring microphones placed near the drone. Experimental validation in a semi-anechoic chamber demonstrates the system's capability to deliver an average noise reduction of 4.78 dB across 1500–2400 Hz within the region of interest, with up to 10 dB attenuation at the drone blade passage frequencies. These findings validate the efficacy of directional ANC strategies in suppressing drone noise and highlight their potential applicability in real-world noise-sensitive environments.

Acknowledgments

H. Bi and Y. Zhang contributed equally to this work.

This research was supported by the Australian Research Council (ARC) Discovery Projects funding schemes with Project No. DP200100693.

Author Declarations

Conflict of Interest

The authors have no conflicts to disclose.

Data Availability

The data that support the findings of this study are available from the corresponding author upon reasonable request.

References

¹<https://github.com/AngelaYZhang/DroneANC>

- Abhayapala, T. D., Birnie, L., Kumar, M., Grixti-Cheng, D., and Samarasinghe, P. N. (2023). "Generalizing the relative transfer function to a matrix for multiple sources and multichannel microphones," in *Proceedings of EUSIPCO*, Helsinki, Finland, pp. 336–340.
- Bi, H., Abhayapala, T., Ma, F., and Samarasinghe, P. N. (2023). "Directional active noise control for drones," *J. Acoust. Soc. Am.* **154**, A162.
- Bi, H., Ma, F., Abhayapala, T. D., and Samarasinghe, P. N. (2021). "Spherical array based drone noise measurements and modelling for drone noise reduction via propeller phase control," in *Proceedings of the Applications of Signal Processing to Audio and Acoustics*, pp. 286–290.
- Bi, H., Ma, F., Abhayapala, T. D., and Samarasinghe, P. N. (2022). "Spherical sector harmonics based directional drone noise reduction," in *Proceedings of the 2022 IWAENC*, Bamberg, Germany, pp. 1–5.
- Chiang, W. C., Li, Y., Shang, J., and Urban, T. L. (2019). "Impact of drone delivery on sustainability and cost: Realizing the UAV potential through vehicle routing optimization," *Appl. Energy* **242**, 1164–1175.
- Christian, A., and Cabell, R. (2017). "Initial investigation into the psychoacoustic properties of small unmanned aerial system noise," in *Proceedings of the 23rd AIAA/CEAS Aeroacoustics Conference*.
- Elliott, S. J., and Nelson, P. A. (1993). "Active noise control," *IEEE Signal Process. Mag.* **10**(4), 12–35.
- Everest, F. A., and Pohlmann, K. C. (2022). *Master Handbook of Acoustics* (McGraw-Hill Education, New York).
- Gur, O., and Rosen, A. (2009). "Design of quiet propeller for an electric mini unmanned air vehicle," *J. Propuls. Power* **25**(3), 717–728.
- Intaratep, N., Alexander, W. N., Devenport, W. J., Grace, S. M., and Dropkin, A. (2016). "Experimental study of quadcopter acoustics and performance at static thrust conditions," in *Proceedings of the 22nd AIAA/CEAS Aeroacoustics Conference*, pp. 1–14.
- Jones, G. P., Pearlstine, L. G., and Percival, H. F. (2006). "An assessment of small unmanned aerial vehicles for wildlife research," *Wildl. Soc. Bull.* **34**(3), 750–758.
- Kuo, S. M., and Morgan, D. R. (1996). *Active Noise Control Systems* (Wiley, New York).
- Kusni, M. (2002). "The active noise control of propeller noise using a multipole secondary source," in *Proceedings of the 23rd ICAS*, Toronto, Canada.
- Luo, Z., Shi, D., Shen, X., and Gan, W.-S. (2024). "Unsupervised learning based end-to-end delayless generative fixed-filter active noise control," in *Proceedings of the 2024 ICASSP*, Seoul, South Korea, pp. 441–445.
- Miljkovic, D. (2018). "Methods for attenuation of unmanned aerial vehicle noise," in *Proceedings of the 41st MIPRO*, pp. 0914–0919.
- Mishra, B., Garg, D., Narang, P., and Mishra, V. (2020). "Drone-surveillance for search and rescue in natural disaster," *Comput. Commun.* **156**, 1–10.
- Narine, M. (2020). "Active noise cancellation of drone propeller noise through waveform approximation and pitch-shifting," Master's thesis, Georgia State University, Atlanta, GA.
- Schiller, N. H., Pascioni, K. A., and Zawodny, N. S. (2019). "Tonal noise control using rotor phase synchronization," in *Proceedings of the 75th Annual Forum of the Vertical Flight Society*, pp. 1–12.
- Shi, D., Lam, B., Ooi, K., Shen, X., and Gan, W.-S. (2022). "Selective fixed-filter active noise control based on convolutional neural network," *Signal Process.* **190**, 108317.
- Steiner, J., Hilgemann, F., and Jax, P. (2025). "Empirical study on active noise control in UAVs," in *Proceedings of the 11th Acusticum*, Málaga, Spain, pp. 1–4.
- Ventura, D., Bruno, M., Jona Lasinio, G., Belluscio, A., and Ardizzone, G. (2016). "A low-cost drone based application for identifying and mapping of coastal fish nursery grounds," *Estuar. Coast. Shelf Sci.* **171**, 85–98.
- Zhang, Y. A., Abhayapala, T. D., Sun, H., Samarasinghe, P. N., and Bastine, A. (2024). "A multi-noise multi-channel ANC system using relative transfer matrix-based approach," in *Proceedings of the 2024 IWAENC*, Aalborg, Denmark, pp. 414–418.